



Year: 2020

FADS3 is a $\Delta 4Z$ sphingoid base desaturase that contributes to gender differences to the human plasma sphingolipidome

Karsai, Gergely ; Lone, Museer ; Kutalik, Zoltán ; Brenna, J Thomas ; Li, Hongde ; Pan, Duoia ; von Eckardstein, Arnold ; Hornemann, Thorsten

Abstract: Sphingolipids (SL) are structurally diverse lipids that are defined by the presence of a long chain base (LCB) backbone. Typically, LCBs contain a single $\Delta 4E$ DB (mostly d18:1), whereas the dienic LCB sphingadienine (d18:2) contains a second DB at $\Delta 14Z$ position. The enzyme introducing the $\Delta 14Z$ DB is unknown. We analyzed the LCB plasma profile in a gender-, age-, and BMI-matched subgroup of the CoLaus cohort ($n = 658$). Sphingadienine levels showed a significant association with gender, being in average 30% higher in females. A genome-wide association study (GWAS) revealed variants in the fatty-acid desaturase 3 (FADS3) gene to be significantly associated with the plasma d18:2/d18:1 ratio ($p = -\log 7.9$). Metabolic labeling assays, FADS3 overexpression and knockdown approaches, as well as plasma LCB profiling in FADS3-deficient mice confirmed that FADS3 is a bona-fide LCB desaturase and required for the introduction of the $\Delta 14Z$ double bond. Moreover, we showed that FADS3 is required for the conversion of the atypical cytotoxic 1-deoxysphinganine (1-deoxySA, m18:0) to 1-deoxysphingosine (1-deoxySO, m18:1). HEK293 cells overexpressing FADS3, were more resistant to m18:0 toxicity than WT cells. In summary, using a combination of metabolic profiling and GWAS, we identified FADS3 to be essential for forming $\Delta 14Z$ DB containing LCBs, such as d18:2 and m18:1. Our results unravel FADS3 as a $\Delta 14Z$ LCB desaturase, thereby disclosing the last missing enzyme of the SL de novo synthesis pathway.

DOI: <https://doi.org/10.1074/jbc.AC119.011883>

Posted at the Zurich Open Repository and Archive, University of Zurich

ZORA URL: <https://doi.org/10.5167/uzh-181692>

Journal Article

Published Version

Originally published at:

Karsai, Gergely; Lone, Museer; Kutalik, Zoltán; Brenna, J Thomas; Li, Hongde; Pan, Duoia; von Eckardstein, Arnold; Hornemann, Thorsten (2020). FADS3 is a $\Delta 4Z$ sphingoid base desaturase that contributes to gender differences to the human plasma sphingolipidome. *Journal of Biological Chemistry*, 295(7):1889-1897.

DOI: <https://doi.org/10.1074/jbc.AC119.011883>

FADS3 is a delta14Z sphingoid base desaturase that contributes to gender differences to the human plasma sphingolipidome

Gergely Karsai¹, Museer Lone¹, Zoltan Kutalik^{2,3}, J. Thomas Brenna⁴, Hongde Li⁵, Duoqia Pan⁵, Arnold von Eckardstein¹, Thorsten Hornemann^{1*}

From the ¹ Institute for Clinical Chemistry, University Hospital and University Zurich, 8091 Zürich, Switzerland; ² University Center for primary care and public health, University of Lausanne, Switzerland; ³ Swiss Institute of Bioinformatics, Lausanne, Switzerland; ⁴ Dell Pediatric Research Institute, Departments of Chemistry, Pediatrics, and Nutrition, University of Texas, 1400 Barbara Jordan Blvd, Austin, Texas 78723, USA; ⁵ Department of Physiology, University of Texas Southwestern Medical Center, Dallas, TX 75390, USA

Running title: FADS3 is a delta14Z sphingoid base desaturase

*To whom correspondence should be addressed: Thorsten Hornemann: Institute for Clinical Chemistry, University Hospital and University Zurich, 8091 Zürich, Switzerland

Keywords: sphingolipid, lipid metabolism, single nucleotide polymorphism (SNP), human genetics, molecular cell biology, fatty-acid desaturase 3 (FADS3), ceramide, GWAS, genomics

ABSTRACT

Sphingolipids (SL) are structurally diverse lipids that are defined by the presence of a long chain base (LCB) backbone. Typically, LCBs contain a single Δ^4 E DB (mostly d18:1), whereas the dienic LCB sphingadienine (d18:2) contains a second DB at Δ^{14} Z position. The enzyme introducing the Δ^{14} Z DB is unknown. We analyzed the LCB plasma profile in a gender-, age-, and BMI-matched subgroup of the CoLaus cohort (n = 658). Sphingadienine levels showed a significant association with gender, being in average ~30% higher in females. A genome-wide association study (GWAS) revealed variants in the fatty-acid desaturase 3 (FADS3) gene to be significantly associated with the plasma d18:2/d18:1 ratio (p=-log 7.9). Metabolic labeling assays, FADS3 overexpression and knockdown approaches, as well as plasma LCB profiling in FADS3-deficient mice confirmed that FADS3 is a bona-fide LCB desaturase and required for the introduction of the Δ^{14} Z double bond. Moreover, we showed that FADS3 is required for the conversion of the atypical cytotoxic 1-deoxysphinganine (1-deoxySA, m18:0) to 1-deoxysphingosine (1-deoxySO, m18:1). HEK293 cells overexpressing FADS3, were more resistant to m18:0 toxicity than WT cells. In summary, using a combination of metabolic profiling and GWAS, we identified FADS3 to be essential for forming Δ^{14} Z DB containing LCBs, such as d18:2 and m18:1. Our results unravel FADS3 as a Δ^{14} Z LCB

desaturase, thereby disclosing the last missing enzyme of the SL *de novo* synthesis pathway.

Introduction

Sphingolipids (SLs) are a diverse class of lipids that share a long-chain base (LCB) backbone as a common structural element. Forming a LCB is the first and rate-limiting reaction in the de-novo synthesis of SL (Fig S1). During SL synthesis, LCBs are usually N-acylated to a fatty acid (FA) of variable length (C16-C26) forming ceramides and conjugated to variable head group structures forming complex SLs. LCBs are synthesized at the endoplasmic reticulum by the enzyme serine-palmitoyltransferase (SPT). The most abundant LCB in mammals is the 18-carbon dihydroxy-amino-alkane sphingosine (d18:1) that is formed by the conjugation of L-serine with palmitoyl-CoA. SPT, however, can metabolize a variety of other acyl-CoA in the range of C₁₄-C₁₈ and use alanine and glycine as alternative substrates. This forms a broad variety of LCBs, which differ by structure, function and metabolism (1). 1-DeoxySLs are atypical SLs, which are generated from alanine instead of serine and involved in a variety of pathological conditions including the rare hereditary sensory neuropathy type 1 (HSAN1) (2). Typically, LCBs present with a canonical Δ^4 E double bond (DB). However, the -dienic sphingoid base sphingadienine (d18:2) that is formed downstream of sphingosine (d18:1) has an additional DB at Δ^{14} Z position (3,4). Recently, we reported that 1-deoxySO (m18:1) contains a

$\Delta 14Z$ DB but lacks the canonical DB at $\Delta 4E$ position (5). Whereas the $\Delta 4E$ DB is introduced by the ceramide desaturase 1 (DEGS1), the enzyme responsible for the introduction of the $\Delta 14Z$ DB is not known. Here we identified fatty-acid desaturase type 3 (FADS3) as a bona fide sphingoid base desaturase introducing a DB in $\Delta 14Z$ position and therefore responsible for converting d18:1 into d18:2 and 1-deoxySA (m18:0) into 1-deoxySO (m18:1).

Results

Human plasma contains different SL classes, of which the most abundant are Sphingomyelins (SM), HexosylCeramides (HexCer) and Ceramides (Cer). These classes are formed on a variety of LCB backbone structures and variations in their LCB composition are associated with different pathological conditions (6-8). Differences in the LCB profile predicts the risk for future diabetes type 2 (T2DM) independent from classical risk factor such as BMI and blood glucose (9). Males and females have different risk profiles for T2DM. In men, T2DM is more frequently diagnosed at lower age and BMI whereas obesity is more common in women. We therefore compared the LCB profile in an age and BMI matched subgroup of female and male participants of the CoLaus cohort (N=329 each). LDL cholesterol, triglycerides and fasting glucose was not different between groups (Table 1) whereas total and HDL cholesterol was higher and waist to hip ratio lower in females ($p = -\log 49.4$). In plasma and tissue, the majority of LCBs is N-acylated and conjugated to variable head groups. Non-conjugated LCBs in plasma are minor and less than 1% of the total. The combination of a variable LCB with a variable FAs frequently results in the formation of isomeric structures (e.g. d18:1/24:0 vs d18:0/24:1) which interfere with the LCB analysis by LC-MS. To avoid interferences with the N-acyl chain, we subjected the extracted lipids to a sequential acid/base hydrolysis (10) to remove the conjugated FA and head groups. Here, we therefore reported total LCB concentrations without considering previously conjugated N-acyl and head group structures.

The LCB profiling revealed d18:1 as the most abundant LCB in plasma (57%) followed by d18:2 (21%), d16:1 (5%) and d17:1 (4.2%). The remaining LCB species were less than 5% in total (Fig 1A). A significant gender differences were seen for d18:2 ($p = -\log 32.3$) followed by d17:1 ($p = -\log 15.5$) and d16:1 ($p = -\log 11.6$) LCBs (Fig

1B). In average, d18:2 was about 30% higher in females, whereas its precursor d18:1 was only 10% increased. This indicates that the d18:1 to d18:2 conversion differs between genders. However, the enzyme responsible for this conversion was not known.

To identify the responsible $\Delta 14Z$ desaturase, we used genome wide SNP data, which were available for all European individuals of the cohort (11). As the enzyme converts d18:1 into d18:2, we hypothesized that genetic variations in the desaturase gene will be reflected by changes in the d18:1 to d18:2 ratio. We therefore used this ratio as a metabolic outcome trait for a GWAS on 1100 participants of the CoLaus cohort of whom the LCB profile was already available from an earlier study (9). The analysis revealed a group of adjacent SNPs, showing a significant association with the d18:1/d18:2 ratio. The strongest association was seen for SNP rs174455 ($p = -\log 7.93$) that is located in an intronic region of the fatty acid desaturase 3 (FADS3) gene on chromosome 11q12.2-13.1 (Fig 1D). The same region clusters two other desaturases, FADS1 and FADS2, which metabolize polyunsaturated fatty acids (PUFA) (12). In contrast, the function of FADS3 was still elusive. The FADS3 gene spans 17.9 kb of genomic DNA and has the same structure as FADS1 and FADS2 consisting of 12 exons and 11 introns. On protein level, FADS3 is 52% and 62% homologous to FADS1 and FADS2, respectively.

To test whether FADS3 is a $\Delta 14Z$ LCB desaturase, we expressed the mouse and human FADS3 cDNA in HEK293 cells. Endogenous d18:2 levels in HEK293 cells were low, indicating a low activity of the putative $\Delta 14Z$ desaturase. For comparison, we also expressed the cDNA of mFADS1 and mFADS2. Expression levels were comparable for all constructs (Fig 2A). Immune fluorescence microscopy showed an intracellular colocalisation of FADS3 with calnexin, indicating that FADS3 is an ER protein (Fig 2B).

Enzyme activity was tested in human and mouse FADS3 expressing cells supplemented either with isotope labelled (d7)d18:0 or (d3)m18:0. The free LCBs were absorbed by the cells (13) and metabolized to (d7)ceramide and downstream products such as (d7)SM and (d7)HexCer (Fig S2A). After 48 hours, the lipids were extracted, hydrolyzed and the LCB profile analyzed by LC-MS. In both, mFADS3 and hFADS3 expressing cells, we observed a strong

increase in d18:2 (Fig 2C, S2B) which was not seen in mFADS1 or mFADS2 expressing cells. In addition, FADS3 expressing cells showed an increased conversion of m18:0 into m18:1, indicating that the $\Delta 14Z$ DB in 1-deoxySO is also formed by FADS3 (Fig 2D, S2C). To test whether FADS3 acts on N-acylated or free LCB, we treated cells with Fumonisin B1 (FB1). FB1 blocks Ceramide Synthase (CerS) and therefore the N-acylation of LCBs. In the presence of FB1, the conversion was about 70% reduced, but a significant amount of (d7)d18:1 was still converted into (d7)d18:2. This was confirmed *in vitro*, by adding either the free LCB (d7)d18:1 or the N-acylated d18:1/6:0 to cell free extract of FADS3 expressing HEK cells. Both, the free and the N-acylated LCBs were effectively converted into their dienic forms (Fig 2F), indicating that FADS3 is capable to metabolize both, free and N-acylated LCBs.

For further confirmation, we performed the reverse experiments by knocking down endogenous FADS3 in HeLa cells, which had a higher endogenous FADS3 expression than HEK293 cells. Transfection with FADS3 siRNA (siFADS3) abolished FADS3 expression almost completely compared to cells transfected with control siRNA (siSCR) (Fig 3A). LCB profiling revealed that, almost no isotope labelled (d7)d18:2 was formed in absence of FADS3, whereas in siSCR treated cells a significant conversion of (d7)d18:0 into (d7)d18:1 and finally into (d7)d18:2 was observed (Fig 3B). Similarly, the conversion of isotope labelled (d3)m18:0 into (d3)m18:1 was mostly abolished in siFADS3 treated cells (Fig 3C, S4).

Finally, we analyzed the LCB profile in plasma of FADS3 deficient mice (14). No d18:2 was detected in plasma of FADS^{-/-} mice whereas FADS^{+/-} mice had about 50% of the wildtype levels (Fig 3D).

To see whether the $\Delta 14Z$ DB has a biological relevance, we cultured WT and FADS3 overexpressing cells with increasing amounts of m18:0 and quantified the number of surviving cells after 48 hours. Hek293 cells overexpressing FADS3 were significantly more resistant to m18:0 toxicity than WT cells (Fig 3F).

As d18:2 plasma levels were higher in females, we compared the FADS3 tissue expression between males and females using the public gene expression data from the GTEx portal (<https://gtexportal.org>). Overall, the highest FADS3 expression was seen for peripheral nerve, aorta and adipose tissue. The majority of tissues

showed higher FADS3 expression in females. The most pronounced difference was seen for adipose tissues with 194.6 transcripts per million (TPM) in females vs 166.7 TPM in males.

Discussion

Sphingadienine (d18:2) is an atypical sphingoid base which contains two DBs, a $\Delta 4E$ and a $\Delta 14Z$ (3,15). Whereas the $\Delta 4E$ DB is introduced by DEGS1 during SL de-novo synthesis, the enzyme introducing the $\Delta 14Z$ DB was not known. However, in a gender, age and BMI matched cohort, we identified d18:2 as the second most abundant LCB (Fig 1A) and significantly higher in females than in males. This confirms data from two recent epidemiologic studies, which also report gender specific difference in d18:2 based SL (16,17).

Although, d18:2 was first described in the late 60's (3), the responsible enzyme forming the $\Delta 14Z$ double was not known. Based on genetic association studies in combination with *in vivo* and *in vitro* experiments, we identified FADS3 as a bona-fide delta $\Delta 14Z$ long chain base desaturase. Data from the GTEx database revealed generally higher FADS3 expression in females for many tissues, including peripheral nerve and adipose tissue but also liver, kidney and muscle. Higher FADS3 expression was also reported for female mice (18) and might explain the gender specific differences in d18:2 plasma levels.

Although, human FADS3 was first cloned in 2000 (19), its function remained elusive. FADS3 is composed of an N-terminal cytochrome b5-like domain and three histidine motifs at the C-terminal ends which is characteristic for membrane-bound front end desaturases (20). *In vitro* studies indicated that FADS3 is specific for trans-vaccenic acid (VA; trans11-18:1), catalyzing the synthesis of a trans11,cis13-linoleic acid isomer ($\Delta 13$ desaturation) (21). Interestingly, an earlier GWAS on genetic determinants of circulating sphingolipids found FADS3 to be strongly associated with SM species containing mono-unsaturated N-acyl chains (22). As d18:1 based SLs with unsaturated acyl chains (e.g. SM d18:1/24:1) are isobaric to SLs with a saturated fatty acids formed on d18:2 backbone (e.g. SM d18:2/24:0), these associations could also refer to –dienic SM species (Fig S3, S5).

FADS3 localizes to human chromosome 11q13 (23) which is known as a cancer hotspot locus (19,24). It is located in a gene cluster

together with FADS1 and FADS2 which were identified previously as delta-5 and delta-6 desaturases. FADS3 mRNA expression responds inversely to FADS1 and FADS2 expression levels. In FADS2 deficient mice, FADS3 expression increased 3-fold (25) and reducing FADS1 and FADS2 expression by DHA and arachidonic acid (ARA) increases expression of FADS3 (26). FADS3 is spliced yielding to alternative transcripts, which are conserved in several mammalian and avian species (18,27). However, it is not yet clear whether these alternative transcripts are catalytically active.

Little is known about the function of d18:2 based SLs. Previously, plasma levels of d18:2 SLs were inversely associated with the incidence for cardiovascular events (8), the body mass index and the HOMA index (28). It serves as a backbone for complex sphingolipids (Fig 1C) and forms -dienic LCB phosphates (SAdienine-1P) (29). Free SAdienes and synthetic analogues exhibit cytotoxic and anti-proliferative effects in cancer and non-cancer cells (30,31) and were associated with the inhibition of colon tumorigenesis in mouse models (32,33). Mitochondrial and cellular pools of d18:2 based ceramides were elevated in embryonic fibroblasts derived from double knockout BAX-BAK mice and a mouse derived immortalized iBMK cell line (34). It is noteworthy that the $\Delta 14$ DB in d18:2 is in cis conformation, introducing a kink into the otherwise straight LCB structure. This might affect the lateral assembly of d18:2 based SLs in biological membranes and could interfere with membrane nano-domain formation and receptor clustering. In first reports, FADS3 KO mice showed no overt phenotype (14). No significant differences in survival, fertility or growth rate were seen. However, FADS3 KO mice were not yet tested under challenged metabolic conditions such as high fat diet. Genetic variants of FADS3 are associated with familial combined hyperlipidemia in the Mexican population (35) and the FADS3 SNP rs174455 was negatively associated with DHA levels in red blood cell phospholipids (36).

1-DeoxySLs are an atypical class of toxic sphingolipids associated with the rare inherited neuropathy HSAN1 (37) and macular telangiectasia type 2 (38). In contrast to canonical LCBs m18:1 contains only a single DB in $\Delta 14Z$ position but lacks the $\Delta 4E$ DB (5). Here we showed, that FADS3 is also responsible for the conversion of m18:0 into m18:1 (Fig 2D, 3C, S2 and S4). In addition, we showed, that FADS3

expressing cells were more resistant to m18:0 toxicity than WT cells (Fig 3E). This supports recent reports, indicating that m18:0 based 1-deoxySL species are more associated with toxic effects than their unsaturated forms (39). In that respect, FADS3 might contribute to a physiological detoxification of 1-deoxySLs.

It is not fully clear yet, whether FADS3 activity is specific for N-acylated LCBs or whether it can also metabolize the free form. After blocking N-acylation with FB1, we still observed a conversion of (d7)d18:1 into (d7)d18:2, albeit at reduced levels (Fig 2D). Also in-vitro assays showed, that FADS3 is capable in converting both, the N-acylated and the free LCB. However, as free LCBs are typically minor, the conversion of free LCBs is likely of limited biological relevance.

We recently reported that, DEGS1 deficiency causes leukodystrophy and peripheral hypomyelination. Which was associated with a pathologically increased formation of saturated dihydroSL species (13) and the formation of an atypical monounsaturated d18:1 isomer. Further analysis showed that this isomer contained a $\Delta 14Z$ DB but lacked the canonical $\Delta 4E$ DB. This suggests that FADS3 can also metabolize saturated d18:0 although the atypical d18:1 ($\Delta 14Z$) isomer was yet only detected under conditions with reduced DEGS1 activity.

In conclusion, we identified FADS3 as a $\Delta 14Z$ LCB desaturase introducing a $\Delta 14Z$ DB into d18:1, and m18:0 based SLs and likely also other LCB substrates. This lights up the last obscure step in the SL *de novo* synthesis pathways, as the enzyme that forms d18:2 was not yet identified. The activity of FADS3 seems to be higher in females and relates to gender specific differences in the plasma sphingolipidome. In addition, we propose that FADS3 could be involved in the detoxification of 1-deoxySLs. However, further studies are required to understand role of FADS3 under physiological and pathophysiological conditions.

Experimental procedures

Approvals The Colaus study was conducted according to the principles expressed in the Declaration of Helsinki and approved by the Institutional Ethics Committee of the University of Lausanne.

Animal studies were approved by the Cornell University Institutional Animal Care and Use Committee (IACUC protocol #2011-0007).

Human samples and genome-wide association scan. Two subgroups of age- and BMI-matched females and males (N=329 each) were selected from the CoLaus cohort (9,40). Genotyping and imputation of the cohort was described previously (41). Briefly, individuals with genotyping inconsistencies, or genotyping efficiency below 90%, were removed. SNPs with genotyping efficiency below 70%, or Hardy-Weinberg p-values smaller than $1E-7$, were removed. Duplicate individuals, and first and second degree relatives, were identified by computing genomic identity-by-descent coefficients, using PLINK (42). Imputation was performed using the method of Marchini et al. (43), using IMPUTE version 0.2.0, CEU haplotypes and fine scale recombination map from HapMap release 21. Given the non-Gaussian distribution of the examined LCBs, inverse normal quantile transformation was applied, regressing out age, sex and the first four ancestry principal components. The residual trait has been rescaled to have zero mean and unit variance. Linear regression analysis has been performed for 2'557'249 imputed genetic markers as explanatory variables. The probabilistic genotypes were converted to allele dosages.

Cells and cell culture. HEK293 and HeLa cells (American Type Culture Collection) were cultured in Dulbecco's Modified Eagle's Medium (DMEM, ThermoFisher Scientific) with 10% FBS and 1% pen/strep (37°C in 5% CO₂). Transfection was done using Lipofectamin 3000 (ThermoFisher Scientific). Transfected cells were cultured under Blasticidin (ThermoFisher Scientific) for selection. hFADS3 and control siRNA was obtained from Origene and transfected with RNAiMAX (ThermoFisher Scientific) according to the manufacturer's protocol.

Immunohistochemistry HeLa cells were transfected and grown for 24h on 15-mm coverslips, fixed in 4% paraformaldehyde (30 min, RT) and washed in PBS. Cells were blocked for 2h in PBS, 5% BSA, 1% NGS and 0.25% Tx-100) and incubated with the primary antibodies overnight, anti-Calnexin antibody (Sigma, C4731) and anti-V5 antibody (BIORAD MCA1360) were used. Secondary antibodies (1:1000, Jackson ImmunoResearch) and DAPI (Invitrogen) was added for 4 hours. Cells were mounted on glass slides with ProLong Diamond Antifade Mountant (Thermo Fisher Scientific). Pictures were acquired on a confocal laser

scanning microscope (Leica SP8; Leica Microsystems, Wetzlar, Germany, HC PL APO CS2 63x N.A. 1.4 oil) at 90.4nm*90.4nm*300nm (x*y*z) resolution and analyzed using Fiji image processing package (44).

Protein isolation and Western blots were carried out as described elsewhere (13).

Cloning FADS1 (NM_013402.4), FADS2 (NM_004265.3) and FADS3 (XM_011545023.2) were amplified from a commercially available cDNA library using the following primers:

FADS1 Forward: caccatgggaacgcgcgtcgagg

FADS1 Reverse: ttggtgaagataggcatctagccag

FADS2 Forward: caccatggggaaggagggaaccag

FADS2 Reverse: ttgtgaaggtaggcgtccag

FADS3 Forward: caccatgggcggcgtcgaggagcc

FADS3 Reverse: ctgatggagtaggcgtccagatg

The PCR product was cloned into the pcDNA3.1 V5-His-TOPO vector (ThermoFisher Scientific) and verified using Sanger sequencing. Myc-DDK tagged mouse FADS1-3 plasmids was commercially available (Origene).

Lipidomics analysis was performed as described previously (13,45) using the internal standards (100 pmol/ml, Avanti Polar Lipids): (d5) 1-desoxymethylsphinganine (m17:0), dihydroceramide (d18:0/12:0), ceramide (d18:1/12:0), (d18:1/12:0), 1-deoxydihydroceramide (m18:0/12:0), 1-deoxyceramide (m18:0/12:0), glucosylceramide (d18:1/8:0) and sphingomyelin (d18:1/12:0).

The plasma LCB profile was analyzed as described previously (10). For quantification (d5) 1-desoxymethylSA (m17:0) was used as internal standard (Avanti Polar Lipids).

Metabolic labelling assay 250,000 Cells were seeded and cultured in 6-well plates to 70%–80% confluence. New medium containing isotope labelled (d3)m18:0, (d7)d18:0 or (d7)d18:1 (Avanti Polar Lipids) was added. After 24 or 48 hours, cells were harvested, counted (Beckman Coulter Vi-Cell XR), pelleted (600 g at 4°C) and stored at –20°C.

Activity assay. FADS3 cell were lysed by sonication and the homogenate centrifuged at 13000g for 5 minutes. For each condition 100 µg lysate in 100 µl PBS + 1mM NAD⁺ were incubate with 500 pmol (d7)d18:1 or d18:1/6:0 for 5min. The products were measured by LC-MS.

Statistical analysis was performed using GraphPad Prism 8. A p-value of less than 0.05 was considered statistically significant.

Acknowledgments: This work was supported by grants from the Swiss National Foundation SNF (31003A/179371) the Hurka and Swiss Life Foundation to T.H. and by the Novartis Foundation to A.v.E. The CoLaus study is supported by research grants from GlaxoSmith Kline, the Faculty of Biology and Medicine of Lausanne and the Swiss National Science Foundation (grants 33CS30-122661, 33CS30-139468 and 33CS30-148401). In addition, we want to thank Peter Vollenweider (CHUV, Lausanne) for his contribution and help on the CoLaus samples as well as Yu Wei for her practical help in the lab.

Conflict of interest: The authors declare that they have no conflicts of interest with the contents of this article.

References

1. Carreira, A. C., Santos, T. C., Lone, M. A., Zupancic, E., Lloyd-Evans, E., de Almeida, R. F. M., Hornemann, T., and Silva, L. C. (2019) Mammalian sphingoid bases: Biophysical, physiological and pathological properties. *Prog Lipid Res* **75**, 100988
2. Lone, M. A., Santos, T., Alecu, I., Silva, L. C., and Hornemann, T. (2019) 1-Deoxysphingolipids. *Biochim Biophys Acta Mol Cell Biol Lipids* **1864**, 512-521
3. Renkonen, O., and Hirvisalo, E. L. (1969) Structure of plasma sphingadienine. *J Lipid Res* **10**, 687-693
4. Renkonen, O. (1970) Presence of sphingadienine and trans-monoenoic fatty acids in ceramide monohexosides of human plasma. *Biochim Biophys Acta* **210**, 190-192
5. Steiner, R., Saied, E. M., Othman, A., Arenz, C., Maccarone, A. T., Poad, B. L., Blanksby, S. J., von Eckardstein, A., and Hornemann, T. (2016) Elucidating the chemical structure of native 1-deoxysphingosine. *J Lipid Res* **57**, 1194-1203
6. Othman, A., Rutti, M. F., Ernst, D., Saely, C. H., Rein, P., Drexel, H., Porretta-Serapiglia, C., Lauria, G., Bianchi, R., von Eckardstein, A., and Hornemann, T. (2012) Plasma deoxysphingolipids: a novel class of biomarkers for the metabolic syndrome? *Diabetologia* **55**, 421-431
7. Othman, A., Saely, C. H., Muendlein, A., Vonbank, A., Drexel, H., von Eckardstein, A., and Hornemann, T. (2015) Plasma 1-deoxysphingolipids are predictive biomarkers for type 2 diabetes mellitus. *BMJ open diabetes research & care* **3**, e000073
8. Othman, A., Saely, C. H., Muendlein, A., Vonbank, A., Drexel, H., von Eckardstein, A., and Hornemann, T. (2015) Plasma C20-Sphingolipids predict cardiovascular events independently from conventional cardiovascular risk factors in patients undergoing coronary angiography. *Atherosclerosis* **240**, 216-221
9. Mwinyi, J., Bostrom, A., Fehrer, I., Othman, A., Waeber, G., Marti-Soler, H., Vollenweider, P., Marques-Vidal, P., Schioth, H. B., von Eckardstein, A., and Hornemann, T. (2017) Plasma 1-deoxysphingolipids are early predictors of incident type 2 diabetes mellitus. *PLoS One* **12**, e0175776
10. Alecu, I., Othman, A., Penno, A., Saied, E. M., Arenz, C., von Eckardstein, A., and Hornemann, T. (2017) Cytotoxic 1-deoxysphingolipids are metabolized by a cytochrome P450-dependent pathway. *J Lipid Res* **58**, 60-71
11. Antiochos, P., Marques-Vidal, P., McDaid, A., Waeber, G., and Vollenweider, P. (2016) Association between parental history and genetic risk scores for coronary heart disease prediction: The population-based CoLaus study. *Atherosclerosis* **244**, 59-65
12. Park, H. G., Park, W. J., Kothapalli, K. S., and Brenna, J. T. (2015) The fatty acid desaturase 2 (FADS2) gene product catalyzes Delta4 desaturation to yield n-3 docosahexaenoic acid and n-6 docosapentaenoic acid in human cells. *FASEB J* **29**, 3911-3919
13. Karsai, G., Kraft, F., Haag, N., Korenke, G. C., Hanisch, B., Othman, A., Suriyanarayanan, S., Steiner, R., Knopp, C., Mull, M., Bergmann, M., Schroder, J. M., Weis, J., Elbracht, M.,

- Begemann, M., Hornemann, T., and Kurth, I. (2019) DEGS1-associated aberrant sphingolipid metabolism impairs nervous system function in humans. *J Clin Invest*
14. Zhang, J. Y., Qin, X., Liang, A., Kim, E., Lawrence, P., Park, W. J., Kothapalli, K. S. D., and Brenna, J. T. (2017) Fads3 modulates docosahexaenoic acid in liver and brain. *Prostaglandins Leukot Essent Fatty Acids* **123**, 25-32
 15. Ryan, E., Nguyen, C. Q. N., Shiea, C., and Reid, G. E. (2017) Detailed Structural Characterization of Sphingolipids via 193 nm Ultraviolet Photodissociation and Ultra High Resolution Tandem Mass Spectrometry. *J Am Soc Mass Spectrom* **28**, 1406-1419
 16. Chew, W. S., Torta, F., Ji, S. S., Choi, H., Begum, H., Sim, X., Khoo, C. M., Khoo, E. Y. H., Ong, W. Y., Van Dam, R. M., Wenk, M. R., Tai, E. S., and Herr, D. R. (2019) Large-scale lipidomics identifies associations between plasma sphingolipids and T2DM incidence. *Jci Insight* **4**
 17. Huynh, K., Barlow, C. K., Jayawardana, K. S., Weir, J. M., Mellett, N. A., Cinel, M., Magliano, D. J., Shaw, J. E., Drew, B. G., and Meikle, P. J. (2019) High-Throughput Plasma Lipidomics: Detailed Mapping of the Associations with Cardiometabolic Risk Factors. *Cell Chem Biol* **26**, 71-84 e74
 18. Pedrono, F., Blanchard, H., Kloareg, M., D'Andrea, S., Daval, S., Rioux, V., and Legrand, P. (2010) The fatty acid desaturase 3 gene encodes for different FADS3 protein isoforms in mammalian tissues. *J Lipid Res* **51**, 472-479
 19. Marquardt, A., Stohr, H., White, K., and Weber, B. H. (2000) cDNA cloning, genomic structure, and chromosomal localization of three members of the human fatty acid desaturase family. *Genomics* **66**, 175-183
 20. Park, W. J., Kothapalli, K. S., Reardon, H. T., Kim, L. Y., and Brenna, J. T. (2009) Novel fatty acid desaturase 3 (FADS3) transcripts generated by alternative splicing. *Gene* **446**, 28-34
 21. Rioux, V., Pedrono, F., Blanchard, H., Duby, C., Boulier-Monthean, N., Bernard, L., Beauchamp, E., Catheline, D., and Legrand, P. (2013) Trans-vaccenate is Delta13-desaturated by FADS3 in rodents. *J Lipid Res* **54**, 3438-3452
 22. Hicks, A. A., Pramstaller, P. P., Johansson, A., Vitart, V., Rudan, I., Ugocsai, P., Aulchenko, Y., Franklin, C. S., Liebisch, G., Erdmann, J., Jonasson, I., Zorkoltseva, I. V., Pattaro, C., Hayward, C., Isaacs, A., Hengstenberg, C., Campbell, S., Gnewuch, C., Janssens, A. C., Kirichenko, A. V., Konig, I. R., Marroni, F., Polasek, O., Demirkan, A., Kolcic, I., Schwienbacher, C., Igl, W., Biloglav, Z., Witteman, J. C., Pichler, I., Zaboli, G., Axenovich, T. I., Peters, A., Schreiber, S., Wichmann, H. E., Schunkert, H., Hastie, N., Oostra, B. A., Wild, S. H., Meitinger, T., Gyllenstein, U., van Duijn, C. M., Wilson, J. F., Wright, A., Schmitz, G., and Campbell, H. (2009) Genetic determinants of circulating sphingolipid concentrations in European populations. *PLoS Genet* **5**, e1000672
 23. Blanchard, H., Legrand, P., and Pedrono, F. (2011) Fatty Acid Desaturase 3 (Fads3) is a singular member of the Fads cluster. *Biochimie* **93**, 87-90
 24. Park, W. J., Kothapalli, K. S., Lawrence, P., and Brenna, J. T. (2011) FADS2 function loss at the cancer hotspot 11q13 locus diverts lipid signaling precursor synthesis to unusual eicosanoid fatty acids. *PLoS One* **6**, e28186
 25. Stroud, C. K., Nara, T. Y., Roqueta-Rivera, M., Radlowski, E. C., Lawrence, P., Zhang, Y., Cho, B. H., Segre, M., Hess, R. A., Brenna, J. T., Haschek, W. M., and Nakamura, M. T. (2009) Disruption of FADS2 gene in mice impairs male reproduction and causes dermal and intestinal ulceration. *J Lipid Res* **50**, 1870-1880
 26. Reardon, H. T., Hsieh, A. T., Park, W. J., Kothapalli, K. S., Anthony, J. C., Nathanielsz, P. W., and Brenna, J. T. (2013) Dietary long-chain polyunsaturated fatty acids upregulate expression of FADS3 transcripts. *Prostaglandins Leukot Essent Fatty Acids* **88**, 15-19
 27. Brenna, J. T., Kothapalli, K. S., and Park, W. J. (2010) Alternative transcripts of fatty acid desaturase (FADS) genes. *Prostaglandins Leukot Essent Fatty Acids* **82**, 281-285
 28. Chew, W. S., Torta, F., Ji, S., Choi, H., Begum, H., Sim, X., Khoo, C. M., Khoo, E. Y. H., Ong, W. Y., Van Dam, R. M., Wenk, M. R., Tai, E. S., and Herr, D. R. (2019) Large-scale lipidomics identifies associations between plasma sphingolipids and T2DM incidence. *JCI Insight* **5**

29. Sutter, I., Velagapudi, S., Othman, A., Riwanto, M., Manz, J., Rohrer, L., Rentsch, K., Hornemann, T., Landmesser, U., and von Eckardstein, A. (2015) Plasmalogens of high-density lipoproteins (HDL) are associated with coronary artery disease and anti-apoptotic activity of HDL. *Atherosclerosis* **241**, 539-546
30. Sugawara, T., Zaima, N., Yamamoto, A., Sakai, S., Noguchi, R., and Hirata, T. (2006) Isolation of sphingoid bases of sea cucumber cerebroside and their cytotoxicity against human colon cancer cells. *Biosci Biotechnol Biochem* **70**, 2906-2912
31. Struckhoff, A. P., Bittman, R., Burow, M. E., Clejan, S., Elliott, S., Hammond, T., Tang, Y., and Beckman, B. S. (2004) Novel ceramide analogs as potential chemotherapeutic agents in breast cancer. *J Pharmacol Exp Ther* **309**, 523-532
32. Symolon, H., Schmelz, E. M., Dillehay, D. L., and Merrill, A. H., Jr. (2004) Dietary soy sphingolipids suppress tumorigenesis and gene expression in 1,2-dimethylhydrazine-treated CF1 mice and ApcMin/+ mice. *J Nutr* **134**, 1157-1161
33. Fyrst, H., Oskouian, B., Bandhuvula, P., Gong, Y., Byun, H. S., Bittman, R., Lee, A. R., and Saba, J. D. (2009) Natural sphingadienes inhibit Akt-dependent signaling and prevent intestinal tumorigenesis. *Cancer Res* **69**, 9457-9464
34. Zhang, T., Barclay, L., Walensky, L. D., and Saghatelian, A. (2015) Regulation of mitochondrial ceramide distribution by members of the BCL-2 family. *J Lipid Res* **56**, 1501-1510
35. Plaisier, C. L., Horvath, S., Huertas-Vazquez, A., Cruz-Bautista, I., Herrera, M. F., Tusie-Luna, T., Aguilar-Salinas, C., and Pajukanta, P. (2009) A systems genetics approach implicates USF1, FADS3, and other causal candidate genes for familial combined hyperlipidemia. *PLoS Genet* **5**, e1000642
36. Koletzko, B., Lattka, E., Zeilinger, S., Illig, T., and Steer, C. (2011) Genetic variants of the fatty acid desaturase gene cluster predict amounts of red blood cell docosahexaenoic and other polyunsaturated fatty acids in pregnant women: findings from the Avon Longitudinal Study of Parents and Children. *Am J Clin Nutr* **93**, 211-219
37. Penno, A., Reilly, M. M., Houlden, H., Laura, M., Rentsch, K., Niederkofler, V., Stoeckli, E. T., Nicholson, G., Eichler, F., Brown, R. H., Jr., von Eckardstein, A., and Hornemann, T. (2010) Hereditary sensory neuropathy type 1 is caused by the accumulation of two neurotoxic sphingolipids. *J Biol Chem* **285**, 11178-11187
38. Gantner, M. L., Eade, K., Wallace, M., Handzlik, M. K., Fallon, R., Trombley, J., Bonelli, R., Giles, S., Harkins-Perry, S., Heeren, T. F. C., Sauer, L., Ideguchi, Y., Baldini, M., Schepke, L., Dorrell, M. I., Kitano, M., Hart, B. J., Cai, C., Nagasaki, T., Badur, M. G., Okada, M., Woods, S. M., Egan, C., Gillies, M., Guymer, R., Eichler, F., Bahlo, M., Fruttiger, M., Allikmets, R., Bernstein, P. S., Metallo, C. M., and Friedlander, M. (2019) Serine and Lipid Metabolism in Macular Disease and Peripheral Neuropathy. *N Engl J Med* **381**, 1422-1433
39. Hannich, J. T., Haribowo, A.G., Gentina, S. et al. . (2019) 1-Deoxydihydroceramide causes anoxic death by impairing chaperonin-mediated protein folding. . *Nat Metab* **1**, 996-1008
40. Firmann, M., Mayor, V., Vidal, P. M., Bochud, M., Pecoud, A., Hayoz, D., Paccaud, F., Preisig, M., Song, K. S., Yuan, X., Danoff, T. M., Stirnadel, H. A., Waterworth, D., Mooser, V., Waeber, G., and Vollenweider, P. (2008) The CoLaus study: a population-based study to investigate the epidemiology and genetic determinants of cardiovascular risk factors and metabolic syndrome. *BMC Cardiovasc Disord* **8**, 6
41. Kutalik, Z., Johnson, T., Bochud, M., Mooser, V., Vollenweider, P., Waeber, G., Waterworth, D., Beckmann, J. S., and Bergmann, S. (2011) Methods for testing association between uncertain genotypes and quantitative traits. *Biostatistics* **12**, 1-17
42. Purcell, S., Neale, B., Todd-Brown, K., Thomas, L., Ferreira, M. A., Bender, D., Maller, J., Sklar, P., de Bakker, P. I., Daly, M. J., and Sham, P. C. (2007) PLINK: a tool set for whole-genome association and population-based linkage analyses. *Am J Hum Genet* **81**, 559-575
43. Marchini, J., Howie, B., Myers, S., McVean, G., and Donnelly, P. (2007) A new multipoint method for genome-wide association studies by imputation of genotypes. *Nat Genet* **39**, 906-913

44. Schindelin, J., Arganda-Carreras, I., Frise, E., Kaynig, V., Longair, M., Pietzsch, T., Preibisch, S., Rueden, C., Saalfeld, S., Schmid, B., Tinevez, J. Y., White, D. J., Hartenstein, V., Eliceiri, K., Tomancak, P., and Cardona, A. (2012) Fiji: an open-source platform for biological-image analysis. *Nat Methods* **9**, 676-682
45. Storti, F., Klee, K., Todorova, V., Steiner, R., Othman, A., van der Velde-Visser, S., Samardzija, M., Meneau, I., Barben, M., Karademir, D., Pauzuolyte, V., Boye, S. L., Blaser, F., Ullmer, C., Dunaief, J. L., Hornemann, T., Rohrer, L., den Hollander, A., von Eckardstein, A., Fingerle, J., Maugeais, C., and Grimm, C. (2019) Impaired ABCA1/ABCG1-mediated lipid efflux in the mouse retinal pigment epithelium (RPE) leads to retinal degeneration. *Elife* **8**

	female			male			
		<i>mean</i>	<i>SD</i>	<i>mean</i>	<i>SD</i>	<i>fold</i> <i>diff</i>	<i>-log(p)</i>
<i>n</i>		329		329			
age		59.77	9.07	58.31	10.52	1.02	1.24
BMI		28.61	5.03	27.82	4.28	1.03	1.50
waist/hip ratio		0.86	0.07	0.94	0.06	0.91	49.39
Chol (total)		5.94	1.09	5.63	0.94	1.06	4.08
HDL		1.66	0.40	1.38	0.31	1.20	21.24
LDL		3.59	0.95	3.51	0.82	1.02	0.66
Trig		1.51	0.70	1.63	0.84	0.93	1.37
Glu		6.02	1.67	6.14	1.79	0.98	0.43
C ₁₆ SO	<i>d16:1</i>	19.63	5.73	16.58	5.21	1.18	11.58
C ₁₆ SA	<i>d16:0</i>	0.51	0.20	0.44	0.18	1.14	4.65
C ₁₇ SO	<i>d17:1</i>	9.52	2.63	7.91	2.28	1.20	15.45
C ₁₈ PhytoSO	<i>t18:0</i>	0.15	0.05	0.14	0.04	1.02	0.47
C ₁₈ SO	<i>d18:1</i>	97.23	19.15	88.32	16.54	1.10	9.45
C ₁₈ SA	<i>d18:0</i>	3.51	1.08	3.12	1.00	1.12	5.48
C ₁₈ SAdienine	<i>d18:2</i>	35.05	7.80	28.01	6.33	1.25	32.26
C ₁₉ SO	<i>d19:1</i>	2.45	0.96	2.16	0.91	1.14	4.12
C ₂₀ SO	<i>d20:1</i>	0.20	0.06	0.19	0.05	1.03	0.57
C ₂₀ SA	<i>d20:0</i>	0.02	0.01	0.02	0.01	1.02	0.28
1-deoxySO	<i>m18:1</i>	0.15	0.08	0.17	0.09	0.85	4.10
1-deoxySA	<i>m18:0</i>	0.08	0.04	0.09	0.04	0.95	0.85

Table 1. Baseline values of clinical parameters and long chain base levels for each group

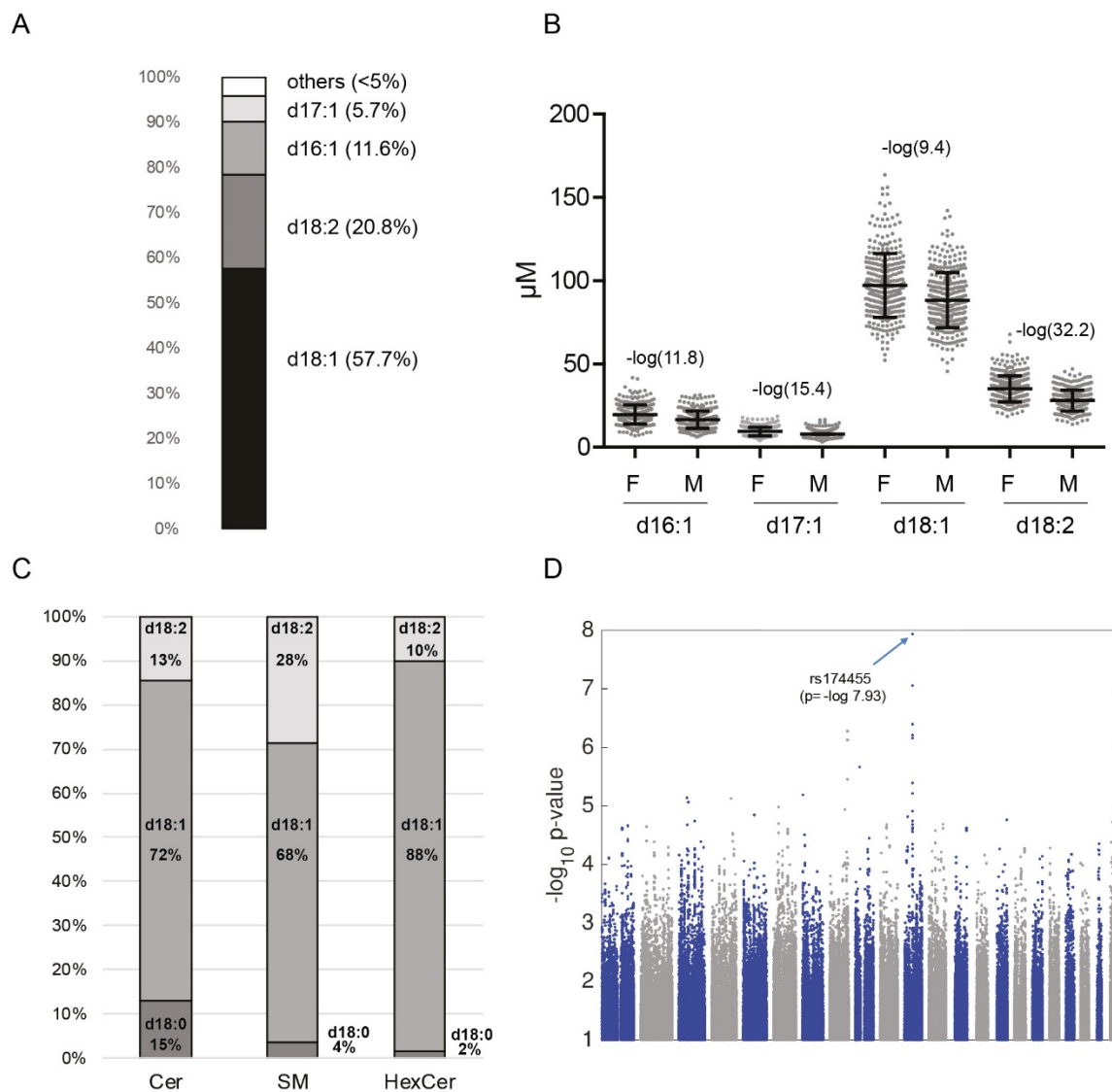


Fig 1. LCB profiling and genetic associations.

A-B Long chain base profile in human plasma. **A** Relative distribution of the most abundant LCBs in human plasma. **B** Differences in the concentration of the major plasma LCBs between females (F) and males (M). **C** Relative distribution of the LCB species d18:0, d18:1 and d18:2 in Ceramide (Cer), HexCer and SM in human plasma. The LCBs reflect the sum of Cer (C16:0, C18:0, C20:0, C22:0, C24:0 and C24:1), SM (C16:0, C18:0, C20:0, C22:0, C24:0 and C24:1) and HexCer (C16:0, C22:0, C24:0 and C24:1) and. **D** Manhattan plot of the GWAS revealed SNP rs174455 on Chromosome 11 to be significantly associated with the d18:1/d18:2 ratio ($p = -\log 7.93$).

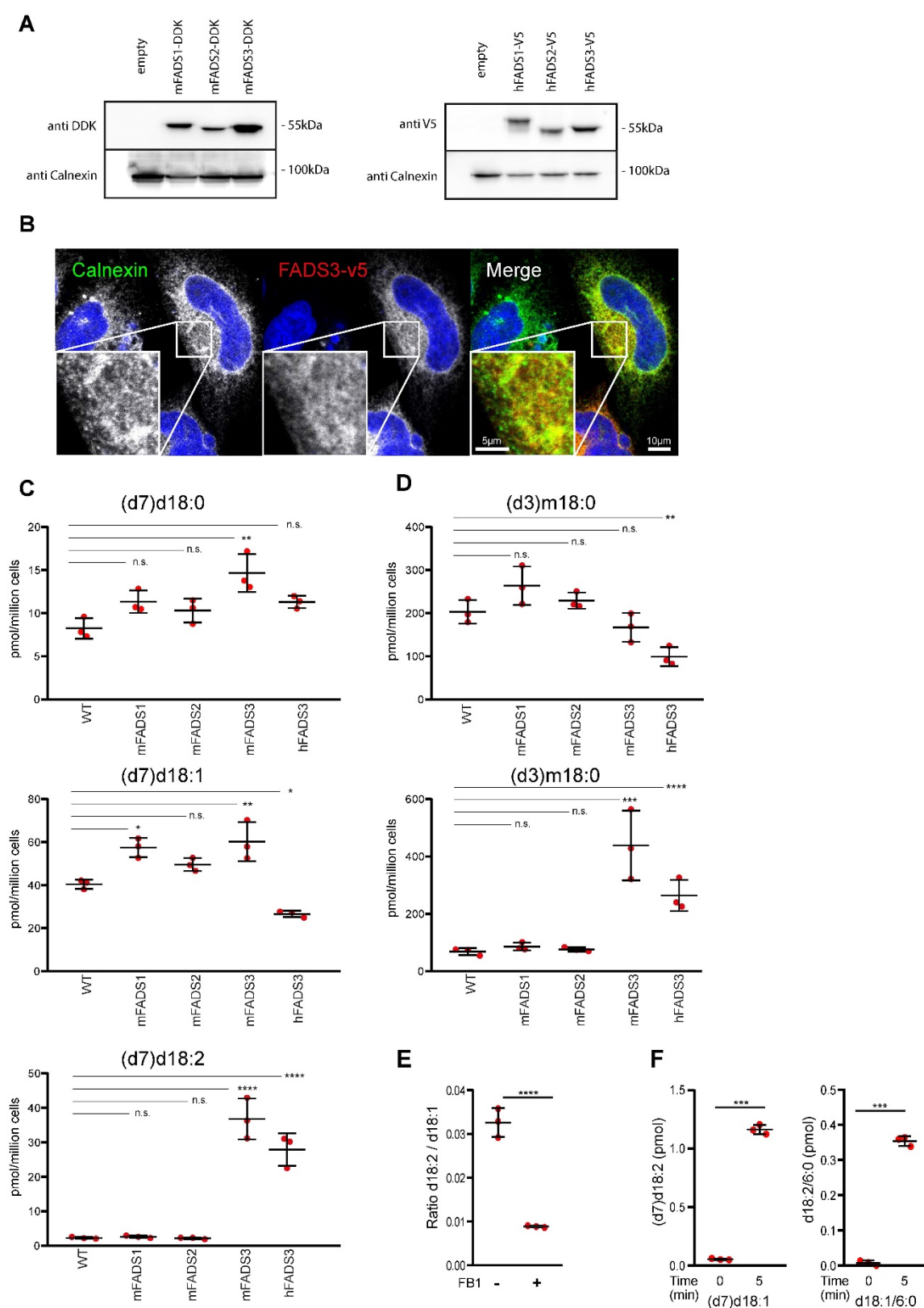


Fig 2. FADS3 mediates the $\Delta 14$ LCB desaturation in mammalian cells.

A Western blot of HEK293 cells stably expressing mouse (m)FADS1-3 (Myc-DDK) and human (h)FADS1-3 (V5) **B** Intracellular localization of hFADS3-V5 (red) overlaps with the ER marker Calnexin (green). Scale bar: 10 μ m. Inserts shows 3-fold magnification. Scale bar: 5 μ m. **C-E** Sphingoid

base profiling of HEK293 cells supplemented with isotope labelled sphingoid bases. **C** Cells stably expressing mFADS1-3 and hFADS3 cultured for 48 hours with isotope-labeled (d7)d18:0. The levels of (d7)d18:2 was significantly elevated in mFADS3 and hFADS3 overexpressing cells but not altered in mFADS1 and mFADS2 cells. **D** FADS1-3 expressing HEK293 cells supplemented with isotope labelled (d3)m18:0 for 48h. (d3)m18:1 levels were higher in FADS3 expressing cells compared to WT, mFADS1 and mFADS2 cells. **E** HEK293 cells supplemented with (d7)d18:1 in the presence or absence of FB1 (35µM). (d7)d18:2 formation was reduced but still detectable in presence of FB1, indicating that FADS3 can also metabolize the free LCB. **F** FADS3 *in-vitro* activity with the free LCB ((d7) d18:1) and the N-acylated form (d18:1/6:0). The free and the N-acylated form were both rapidly converted into (d7)d18:2 and d18:2/6:0, respectively. Data shown as mean±SD, n=3, paired t-test, ***P < 0.001; ****P < 0.0001)

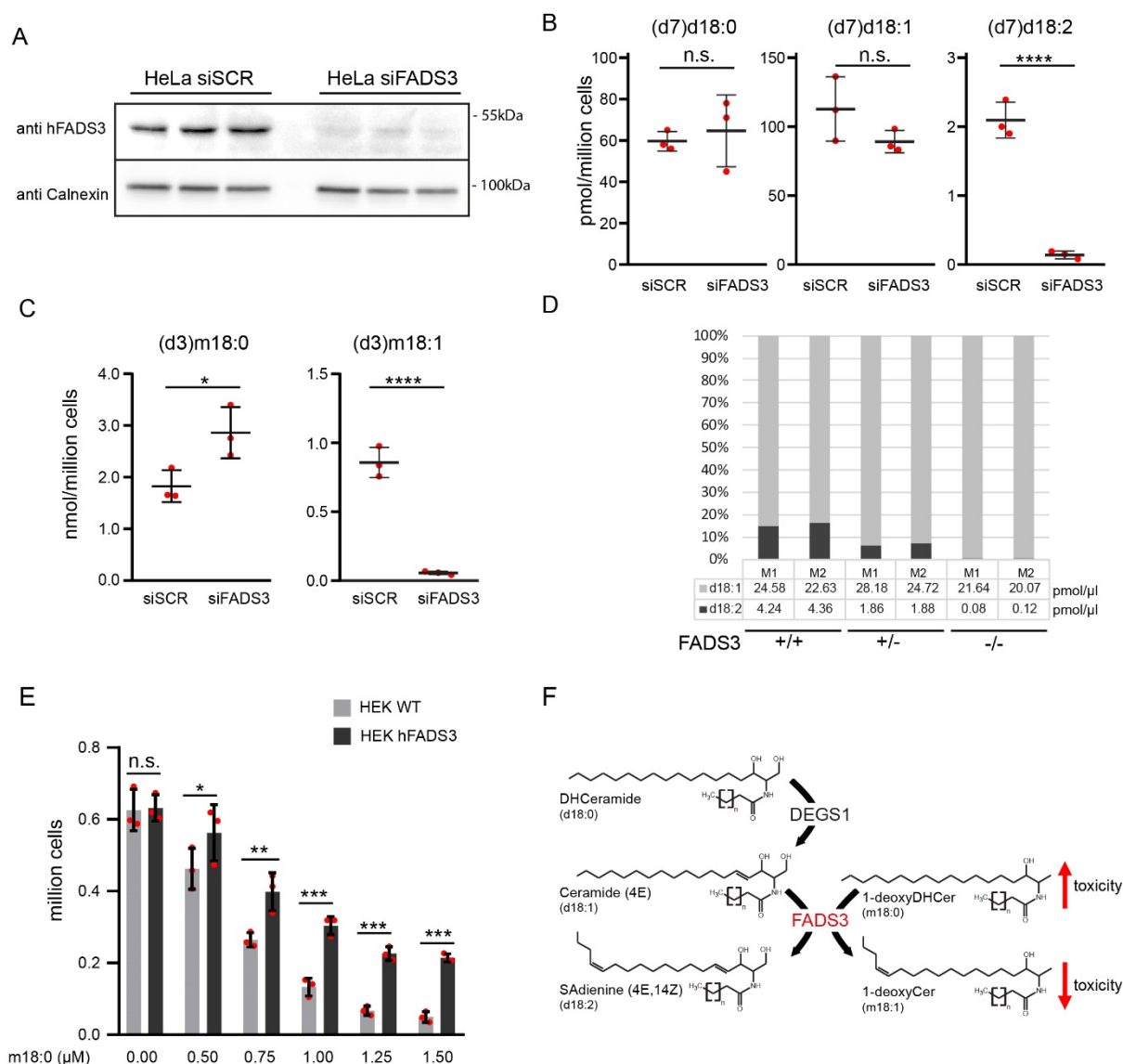


Fig 3. FADS3 is required for $\Delta 14$ LCB desaturation.

A HeLa cells were transfected with hFADS3 siRNA (siFADS3) or scrambled control siRNA (siSCR). The silencing of hFADS3 was confirmed by western blot with a polyclonal antibody against FADS3. Calnexin was used as a loading control (n=3). **B-D** Sphingoid base profiling of cells and plasma. **B** HeLa cells were transfected with siSCR and siFADS3 for 72 hours and subsequently cultured for 24 hours in the presence of 2 μ M (d7)d18:0 and (d3)m18:0. The formation of (d7)d18:2 was significantly decreased in the siFADS3 treated cells. No difference was seen for the precursors (d7)d18:0 and (d7)d18:1. **C** The conversion of (d3)m18:0 into (d3)m18:1 was also reduced in siFADS3 treated cells compared to controls (siSCR). Data shown as mean \pm SD, unpaired t-test, *P < 0.05, ****P < 0.001 **D** d18:2 was absent in plasma of the two FADS (-/-) mice (M1/M2), and about 50% in the FADS (+/-) mice compared to WT. Total d18:1 levels were not different. **E** WT and FADS3 overexpressing HEK293 cells were plated at low density (150 000 cells/well of 24 well plate) and supplemented with increasing concentrations of m18:0 (0-1.5 μ M). After 48 hours, the number of attached cells was significantly higher in FADS3 overexpressing cells than in WT. Data shown as mean \pm SD (n=3) and compared by two-way ANOVA with Bonferroni's correction *P < 0.05, **P < 0.01, ***P < 0.001. **F** Interplay between the two LCB desaturases DEGS1 and FADS3. DEGS1 introduces the $\Delta 4E$ DB into d18:0 forming d18:1, while FADS3 introduces the $\Delta 14Z$ DB into d18:1 and m18:0.

FADS3 is a delta14Z sphingoid base desaturase that contributes to gender differences to the human plasma sphingolipidome

Gergely Karsai, Museer A Lone, Zoltán Kutalik, J Thomas Brenna, Hongde Li, Duoia Pan, Arnold von Eckardstein and Thorsten Hornemann

J. Biol. Chem. published online December 20, 2019

Access the most updated version of this article at doi: [10.1074/jbc.AC119.011883](https://doi.org/10.1074/jbc.AC119.011883)

Alerts:

- [When this article is cited](#)
- [When a correction for this article is posted](#)

[Click here](#) to choose from all of JBC's e-mail alerts